Supporting information

Insights into the synergistic effect of multi-walled carbon nanotubes decorated Mo-doped MoP_2 hybrid electrocatalysts toward efficient and durable overall water splitting

Aijian Wang*[,a], Xiaodong Chen[a], Laixiang Cheng[a], Xiaoliang Shen[a], Weihua Zhu*[,a], Longhua Li[a], Jingyu Pang[b]

[a] School of Chemistry & Chemical Engineering, Jiangsu University, Zhenjiang 212013, P.R. China

[b] Key Laboratory of Polyoxometalate Chemistry of Henan Province, Institute of Molecular and Crystal Engineering, Henan University, Kaifeng 475004, PR China

Methods

The present first principle DFT calculations are performed by Vienna Ab initio Simulation Package(VASP) [1] with the projector augmented wave (PAW) method [2]. The exchange-functional is treated using the generalized gradient approximation (GGA) of Perdew-Burke-Ernzerhof (PBE) [3] functional. The cut-off energy of the plane-wave basis is set at 500 eV for optimize calculations of atoms and cell optimization. The vacuum spacing in a direction perpendicular to the plane of the catalyst is at least 15 Å. The Brillouin zone integration is performed using 3×3×1 Monkhorst-Pack k-point sampling for a primitive cell [4]. The self-consistent calculations apply a convergence energy threshold of 10^{-5} eV. The equilibrium lattice constants are optimized with maximum stress on each atom within 0.05 eV/Å. The Hubbard *U* (DFT+*U*) corrections for 3d transition metal by setting according to the literature [4]. The OER reaction is considered , as below:

$$* + H_2O\ (l) \rightarrow OH^* + H^+ + e^- \quad (1)$$

$$OH^* \rightarrow O^* + H^+ + e^- \quad (2)$$

$$O^* + H_2O\ (l) \rightarrow OOH^* + H^+ + e^- \quad (3)$$

$$OOH^* \rightarrow O_2\ (g) + H^+ + e^- \quad (4)$$

where * is an adsorption site on catalysts. l and g is liquid and gas phases, respectively. Therefore, the ΔG for each step can be calculated by:

$\Delta G_1 = G(OH^*) + G(H^+ + e^-) - G(H_2O) - G(^*)$

$= \{\Delta G_{OH^*} + G(^*) + [G(H_2O) - 1/2G(H_2)]\} + 1/2G(H_2) - G(H_2O) - G(^*)$

$= \Delta G_{OH^*}$

$\Delta G_2 = G(O^*) + G(H^+ + e^-) - G(OH^*)$

$= \{\Delta G_{O^*} + G(^*) + [G(H_2O) - G(H_2)]\} + 1/2G(H_2) - \{\Delta G_{OH^*} + G(^*) + [G(H_2O) - 1/2G(H_2)]\}$

$= \Delta G_{O^*} - \Delta G_{OH^*}$

$\Delta G_3 = G(OOH^*) + G(H^+ + e^-) - G(O^*) - G(H_2O)$

$= \{\Delta G_{OOH^*} + G(^*) + [2G(H_2O) - 3/2G(H_2)]\} + 1/2G(H_2) - \{\Delta G_{O^*} + G(^*) + [G(H_2O) - 1G(H_2)]\} - G(H_2O)$

$= \Delta G_{OOH^*} - \Delta G_{O^*}$

$\Delta G_4 = G(O_2) + G(H^+ + e^-) - G(OOH^*)$

$= \{4.92 + 2G(H_2O) - 2G(H_2)\} + 1/2G(H_2) - \{\Delta G_{OOH^*} + G(^*) + [2G(H_2O) - 3/2G(H_2)]\}$

$= 4.92 - \Delta G_{OOH^*}$

Then the free energies can be obtained by including the zero point energy (ZPE) and the entropy (S) corrections in equation $G=E_{ads}-E_{ZPE}-TS$, The E_{ZPE} could be obtained from the calculation of vibrational frequencies for the adsorbed species.

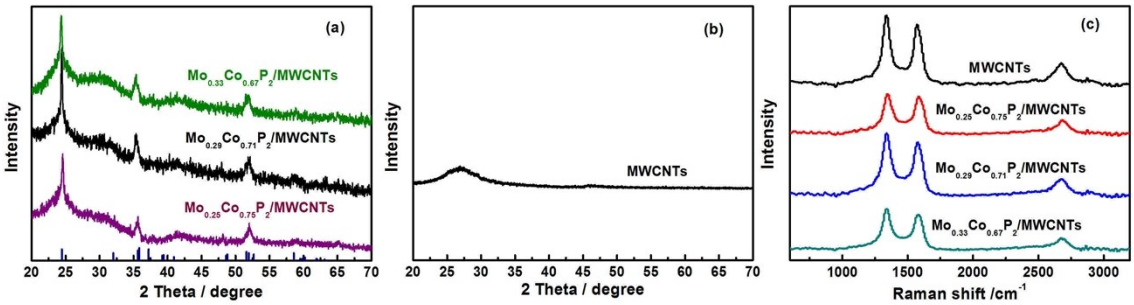

Figure S1. (a, b) XRD patterns and (c) Raman spectra of the as-prepared samples.

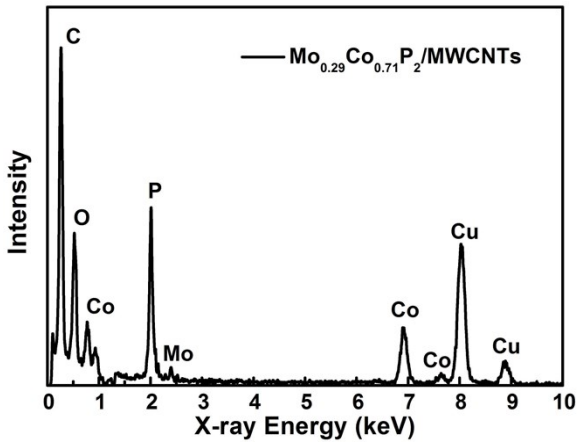

Figure S2. Energy-dispersive X-ray image of $Mo_{0.29}Co_{0.71}P_2$/MWCNTs.

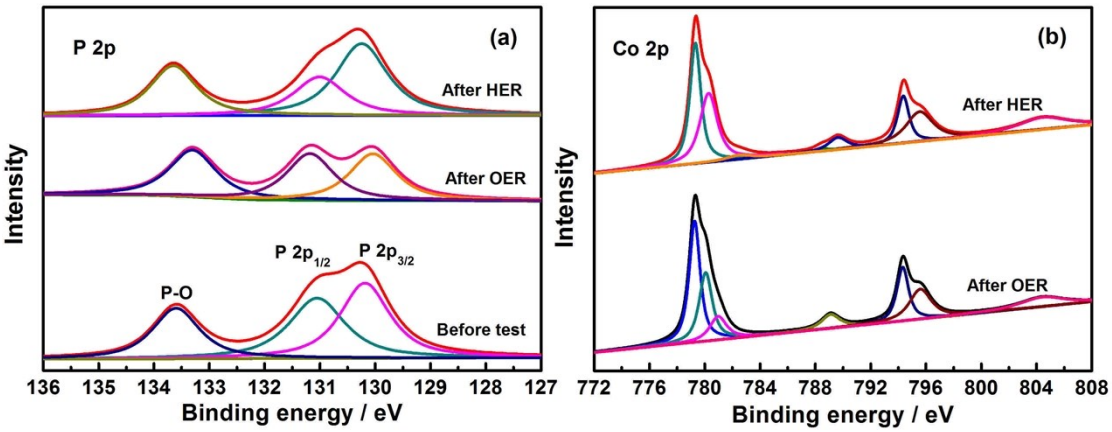

Figure S3. XPS spectra of $Mo_{0.29}Co_{0.71}P_2$/MWCNTs before and after HER and OER test: (a) P 2p and (b) Co 2p.

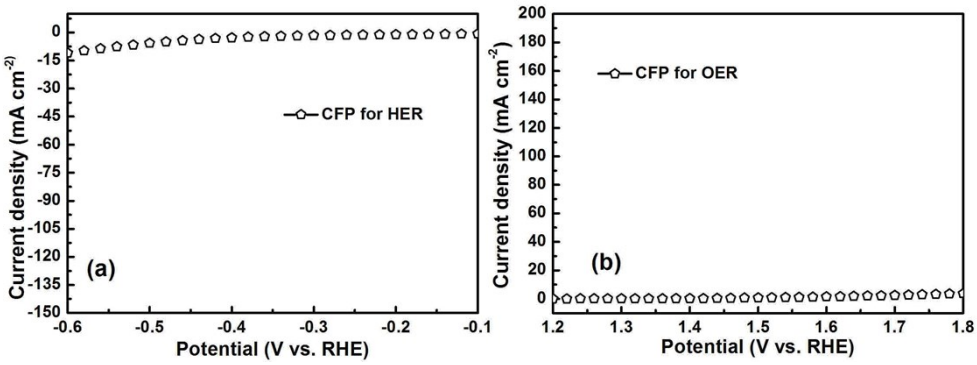

Figure S4. Polarization curves of (a) HER and (b) OER for pure CFP.

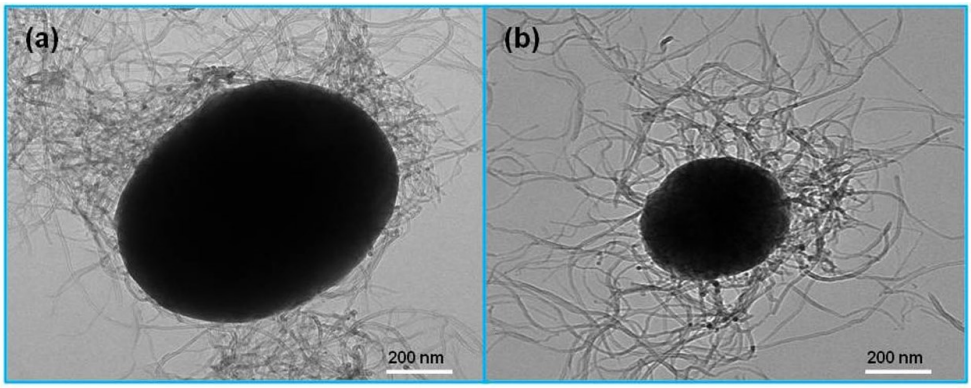

Figure S5. TEM images of $Mo_{0.29}Co_{0.71}P_2$/MWCNTs after (a) HER and (b) OER test.

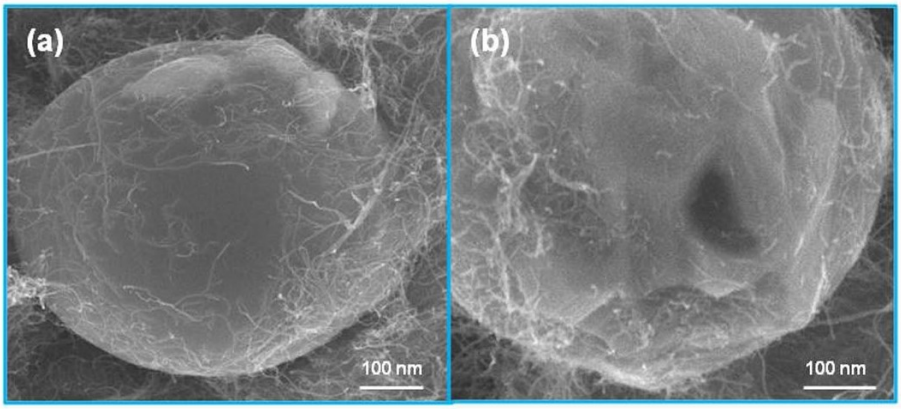

Figure S6. SEM images of $Mo_{0.29}Co_{0.71}P_2$/MWCNTs after (a) HER and (b) OER test.

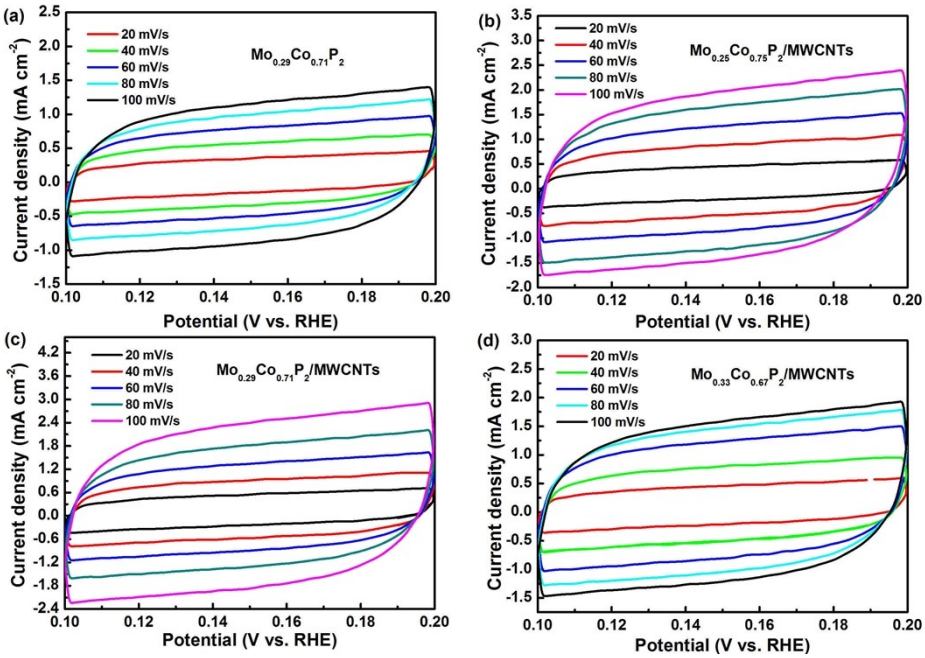

Figure S7. CV curves of the as-prepared samples measured from 20 to 100 mV/s in the non-Faradic region.

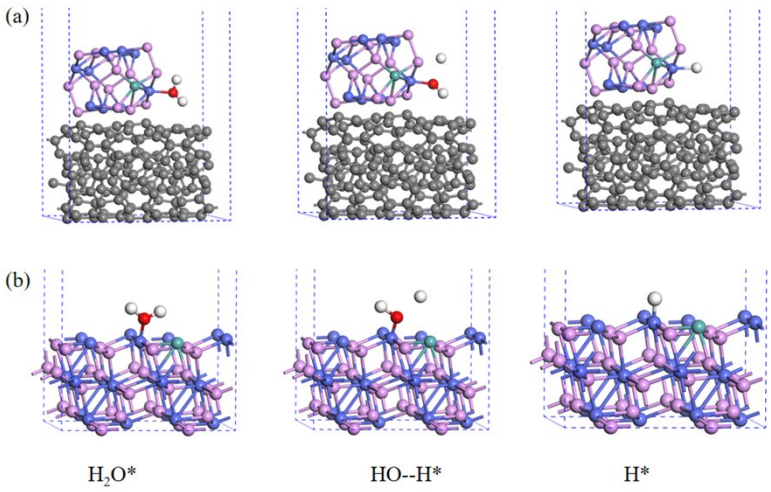

Figure S8. DFT-optimized structures of (a) $Mo_{0.29}Co_{0.71}P_2$/MWCNTs and (b) $Mo_{0.29}Co_{0.71}P_2$ for HER process.

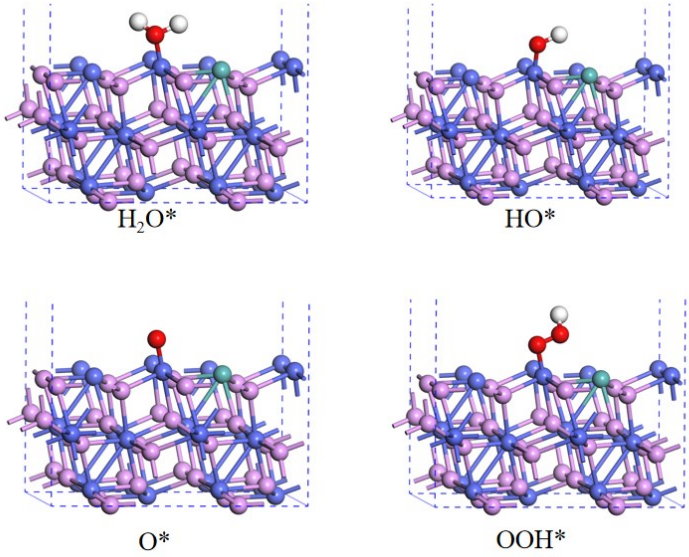

Figure S9. DFT-optimized structures of $Mo_{0.29}Co_{0.71}P_2$ for OER process.

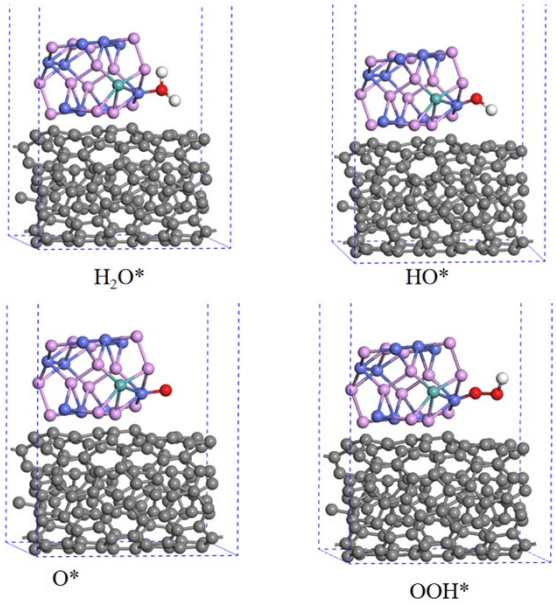

Figure S10. DFT-optimized structures of $Mo_{0.29}Co_{0.71}P_2$/MWCNTs for OER process.

Table S1. Comparison of HER performance of $Mo_{0.29}Co_{0.71}P_2$/MWCNTs with some other reported electrocatalysts in alkaline electrolyte.

Electrocatalysts	Overpotential (mV@10 mA cm^{-2})	Ref.
CoP_3/CoMoP-5/NF	110	5
NiCoP/rGO	209	6
$Cu_{0.3}Co_{2.7}P$/NC	220	7
NiCoN/C nanocages	103	8
Co_2P/CNT-900	132	9
Ni-Mo/Cu nanowires	107	10
MoP/Ni_2P	100.2	11
Co_2P/Co- Foil	112	12
Co_2P@N, P-PCN/CNTs	154	13
CoP/NCNHP	115	14
S:Co_2P NPs	184	15
Co/CoP-HNC	180	16
$Mo_{0.29}Co_{0.71}P_2$/MWCNTs	**84**	**This work**

Table S2. Comparison of OER performance of $Mo_{0.29}Co_{0.71}P_2$/MWCNTs with other reported electrocatalysts in alkaline electrolyte.

Electrocatalysts	Overpotential (mV@10 mA cm^{-2})	Ref.
R-CoP_x/rGO(O)	268	17
Co/CoP	283	18
NiCoP/C	330	19
MoS_2-Co_9S_8-NC	230	20
CoMnP nanoparticles	330	21
NiCoP	280	22
CoP_x/N-doped carbon	319	23
Co_2P–Co_3O4	265 (20 mA cm^{-2})	24
NiCoP films	360	25
NiFe/ Co_9S_8/Carbon Cloth	219	26
Co@Co_9S_8	285	27
$CoFe_2O_4$@NF	250	28
$Mo_{0.29}Co_{0.71}P_2$/MWCNTs	**220**	**This work**

Table S3. The fitting results of EIS spectra.

Sample	R_s (Ω)	R_{ct} (Ω)	CPE	n
$Mo_{0.29}Co_{0.71}P_2$	4.52	30.94	0.015	0.73
$Mo_{0.25}Co_{0.75}P_2$/MWCNTs	2.61	4.56	0.011	0.78
$Mo_{0.29}Co_{0.71}P_2$/MWCNTs	2.41	3.24	0.010	0.91
$Mo_{0.33}Co_{0.67}P_2$/MWCNTs	2.49	6.98	0.013	0.98

Table S4. Comparison of the overall water splitting performance of $Mo_{0.29}Co_{0.71}P_2$/MWCNTs with other reported electrocatalysts in alkaline electrolyte.

Electrocatalysts	Cell voltage (V@10 mA cm^{-2})	Ref.
$Ni_{0.3}Co_{0.7}$-9AC-AD	1.56	29
Ni_2Cr_1 LDH NSA	1.55	30
NiCoP@NC	1.59	31
Holey NiCoP NS	1.56	32
CoP@3D MXene	1.58	33
Co/CoP-HNC	1.68	16
NiCoP/CC	1.52	34
CoP/NC-CNT	1.63	35
Oxidized CoP	1.59	36
MoP/Ni_2P	1.55	11
NiCoP	1.58	22
CoP@NPCSs	1.64	37
CoP/NCNHP	1.64	14
Fe-CoP/Ti	1.60	38
Mo-doped CoP	1.57	39
$Mo_{0.29}Co_{0.71}P_2$/MWCNTs	**1.48**	**This work**

References

[1] Perdew J P, Burke K, Ernzerhof M. Generalized gradient approximation made simple. Phys. Rev. Lett. 1996, 77(18): 3865-3868.

[2] Kresse G, Joubert D P. From ultrasoft pseudopotentials to the projector augmented-wave method. Phys. Rev. B, 1999, 59(3): 1758-1775.

[3] Monkhorst H J, Pack J D. Special points for Brillouin-zone integrations. Phys. Rev. B, 1976, 13(12): 5188-5192.

[4] Gong L L, Zhang D T, Lin C Y, Zhu Y H, Shen Y, Zhang J, Han X, Zhang L P, Xia Z H. Catalytic mechanisms and design principles for single-atom catalysts in highly efficient CO_2 conversion. Adv. Energy Mater. 2019, 9(44): 1902625.

[5] Jiang D L, Xu Y, Yang R, Li D, Meng S C, Chen M. CoP_3/CoMoP heterogeneous nanosheet arrays as robust electrocatalyst for pH-universal hydrogen evolution reaction. ACS Sustain. Chem. Eng., 2019, 7(10): 9309-9317.

[6] Li J Y, Yan M, Zhou X M, Huang Z Q, Xia Z M, Chang C R, Ma Y Y, Qu Y Q. Mechanistic insights on ternary $Ni_{2-x}Co_xP$ for hydrogen evolution and their hybrids with graphene as highly efficient and robust catalysts for overall water splitting. Adv. Funct. Mater., 2016, 26(37): 6785-6796.

[7] Song J H, Zhu C Z, Xu B Z, Fu S F, Engelhard M H, Ye R F, Du D, Beckman S P, Lin Y H, Bimetallic cobalt-based phosphide zeolitic imidazolate framework: CoPx hase-dependent electrical conductivity and hydrogen atom adsorption energy for efficient overall water splitting, Adv. Energy Mater. 2017, 7, 1601555.

[8] Lai, J, Huang B, Chao Y, Chen X, Guo S. Strongly coupled nickel-cobalt nitrides/carbon hybrid nanocages with Pt-like activity for hydrogen evolution catalysis. Adv. Mater. 2019, 31, 1805541.

[9] Das D, Nanda K K. One-step, integrated fabrication of Co_2P nanoparticles encapsulated N, P dual-doped CNTs for highly advanced total water splitting. Nano Energy, 2016: 303-311.

[10] Zhao S N, Huang J F, Liu Y Y, Shen J H, Wang H, Yang X L, Zhu Y H, Li C Z. Multimetallic Ni-Mo/Cu nanowires as nonprecious and efficient full water splitting catalys. J. Mater. Chem. A, 2017, 5(8): 4207-4214.

[11] Du C C, Shang M X, Mao J X, Song W B. Hierarchical MoP/Ni_2P heterostructures on nickel foam for efficient water splitting. J. Mater. Chem. A, 2017, 5(30): 15940-15949.

[12] Yuan C Z, Zhong S L, Jiang Y F, Yang Z K, Zhao Z W, Zhao S J, Jiang N, Xu A W. Direct growth of cobalt-rich cobalt phosphide catalysts on cobalt foil: an efficient and self-supported bifunctional electrode for overall water splitting in alkaline media. J. Mate. Chem. A, 2017, 5(21): 10561-10566.

[13] Li X Z, Fang Y Y, Li F, Tian M, Long X F, Jin J, Ma J T. Ultrafine Co_2P nanoparticles encapsulated in nitrogen and phosphorus dual-doped porous carbon nanosheet/carbon nanotube hybrids: high-performance bifunctional electrocatalysts for overall water splitting. J. Mater. Chem. A, 2016, 4(40): 15501-15510.

[14] Pan Y, Sun K, Liu S, Cao X, Wu K, Cheong W C, Chen Z, Wang Y, Li Y, Liu Y, Wang D, Peng Q, Chen C, Li Y. Core-shell ZIF-8@ZIF-67-derived CoP nanoparticle-

embedded N-doped carbon nanotube hollow polyhedron for efficient overall water splitting. J. Am. Chem. Soc., 2018, 140(7): 2610-2618.

[15] Anjum M A R, Bhatt M D, Lee M H, Lee J S. Sulfur-doped dicobalt phosphide outperforming precious metals as a bifunctional electrocatalyst for alkaline water electrolysis. Chem. Mater., 2018, 30(24): 8861-8870.

[16] Hao Y C, Xu Y Q, Liu W, Sun X M. Co/CoP embedded in a hairy nitrogen-doped carbon polyhedron as an advanced tri-functional electrocatalyst. Mater. Horiz., 2018, 5(1): 108-115.

[17] Zhou X C, Gao H, Wang Y F, Liu Z, Lin J Q, Ding Y. P vacancies-enriched 3D hierarchical reduced cobalt phosphide as a precursor template for defect engineering for efficient water oxidation. J. Mater. Chem. A, 2018, 6(30): 14939-14948.

[18] Xue Z H, Su H, Yu Q Y, Zhang B, Wang H H, Li X H, Chen J S. Janus Co/CoP nanoparticles as efficient Mott–Schottky electrocatalysts for overall water splitting in wide pH range. Adv. Energy Mater., 2017, 7(12): 1602355.

[19] He P L, Yu X Y, Lo X W. Carbon-incorporated nickel-cobalt mixed metal phosphide nanoboxes with enhanced electrocatalytic activity for oxygen evolution. Angew. Chem. 2017, 129, 3955-3958.

[20] Huang N, Yan S F, Zhang M Y, Ding Y Y, Yang L, Sun P P, Sun X H. A MoS_2-Co_9S_8-NC heterostructure as an efficient bifunctional electrocatalyst towards hydrogen and oxygen evolution reaction. Electrochim. Acta, 2019, 327: 134942.

[21] Li D, Baydoun H, Verani C N, Brock S L. Efficient water oxidation using CoMnP nanoparticles. J. Am. Chem. Soc., 2016, 138(12): 4006-4009.

[22] Liang H, Gandi A N, Anjum D H, Wang X, Schwingenschlogl U, Alshareef H N. Plasma-assisted synthesis of NiCoP for efficient overall water splitting. Nano Lett., 2016, 16(12): 7718-7725.

[23] You B, Jiang N, Sheng M L, Gul S, Yano J, Sun Y J, . High-performance overall water splitting electrocatalysts derived from cobalt-based metal–organic frameworks. Chem. Mater., 2015, 27(22): 7636-7642.

[24] Yu X T, Wang M Y, Gong X Z, Guo Z C, Wang Z, Jiao S Q, Self-supporting porous CoP-based films with phase-separation structure for ultrastable overall water electrolysis at large current density, Adv. Energy Mater. 2018, 8: 1802445.

[25] Jothi V R, Bose R, Rajan H, Jung C Y, Yi S C. Harvesting electronic waste for the development of highly efficient eco-design electrodes for electrocatalytic water splitting. Adv. Energy Mater., 2018, 8(34): 1802615.

[26] Zhan C H, Liu Z, Zhou Y, Guo M L, Zhang X L, Tu J C, Ding L, Cao Y. Triple hierarchy and double synergies of NiFe/Co_9S_8/carbon cloth: a new and efficient electrocatalyst for the oxygen evolution reaction. Nanoscale, 2019, 11(7): 3378-3385.

[27] Yuan X, Yin J, Liu Z, Wang X, Dong C, Dong W, Riaz M S, Zhang Z, Chen M Y, Huang F. Charge transfer promoted high oxygen evolution activity of Co@Co_9S_8 core-shell nanochains. ACS Appl. Mater. Interf., 2018, 10(14): 11565-11571.

[28] Urbain F, Du R F, Tang P Y, Smirnov V, Andreu T, Finger F, Divins N J, Llorcs J, Arbiol J, Cabot A, Morante J R. Upscaling high activity oxygen evolution catalysts based on $CoFe_2O_4$ nanoparticles supported on nickel foam for power-to-gas electrochemical conversion with energy efficiencies above 80%. Appl. Catal. B-Environ., 2019, 259: 118055.

[29] Ye W, Yang Y S, Fang X Y, Arif M, Chen X B, Yan D P. 2D cocrystallized metal-organic nanosheet array as an efficient and stable bifunctional electrocatalyst for overall water splitting. ACS Sustain. Chem. Eng., 2019, 7(21): 18085-18092.

[30] Ye W, Fang X Y, Chen X B, Yan D P. A three-dimensional nickel–chromium layered double hydroxide micro/nanosheet array as an efficient and stable bifunctional electrocatalyst for overall water splitting. Nanoscale, 2018, 10(41): 19484-19491.

[31] Yan L T, Cao L, Dai P C, Gu X, Liu D D, Li L J, Wang Y, Zhao X B. Metal-organic frameworks derived nanotube of nickel–cobalt bimetal phosphides as highly efficient electrocatalysts for overall water splitting. Adv. Funct. Mater., 2017, 27(40): 1703455

[32] Fang Z W, Peng L L, Qian Y M, Zhang X, Xie Y J, Cha J J, Yu G H. Dual Tuning of Ni-Co-A (A = P, Se, O) nanosheets by anion substitution and holey engineering for efficient hydrogen evolution. J. Am. Chem. Soc., 2018, 140(15): 5241-5247.

[33] Xiu L Y, Wang Z Y, Yu M Z, Qiu J S. Aggregation-resistant 3D MXene-based architecture as efficient bifunctional electrocatalyst for overall water splitting. ACS Nano, 2018, 12(8): 8017-8028.

[34] Du C, Yang L, Yang F L, Cheng G Z, Luo W. Nest-like NiCoP for highly efficient overall water splitting. ACS Catalysis, 2017, 7(6): 4131-4137.

[35] Guan C, Wu H J, Ren W N, Yang C H, Liu X M, Ouyang X F, Song Z Y, Zhang Y Z, Pennycook S J, Cheng C W, Wang J. Metal-organic framework-derived integrated nanoarrays for overall water splitting. J. Mater. Chem. A, 2018, 6(19): 9009-9018.

[36] Chang J F, Xiao Y, Xiao M L, Ge J J, Liu C P, Xing W. Surface oxidized cobalt-phosphide nanorods as an advanced oxygen evolution catalyst in alkaline solution. ACS Catal., 2015, 5(11): 6874-6878.

[37] Wu K L, Chen Z, Cheong W C, Liu S J, Zhu W, Cao X, Sun K A, Lin Y, Zheng L R, Yan W S, Pan Y, Wang D S, Peng Q, Chen C, Li Y D. Toward bifunctional overall water splitting electrocatalyst: General preparation of transition metal phosphide nanoparticles decorated N-doped porous carbon spheres. ACS Appl. Mate. Interf., 2018, 10(51): 44201-44208.

[38] Tang C, Zhang R, Lu W, He L, Jiang X, Asiri A M, Sun X. Fe-doped CoP nanoarray: A monolithic multifunctional catalyst for highly efficient hydrogen generation, Adv. Mater. 2017, 29,1602441.

[39] Guan C, Xiao W, Wu H J, Liu X M, Zang W J, Zhang H, Ding J, Feng Y P, Pennycook S J, Wang J. Hollow Mo-doped CoP nanoarrays for efficient overall water splitting. Nano Energy, 2018: 73-80.